Indian Journal of Chemical Technology
Vol. 30, July 2023, pp. 492-505
DOI: 10.56042/ijct.v30i4.71465

Investigation of Laurus Tamala leaves extract as an environmentally acceptable corrosion inhibitor for soft steel in 1M HCl: Electrochemical, DFT, and surface characterization techniques

Ragini L Minagalavar[1], S K Rajappa[1]* , Manohar R Rathod[1] & Ashok M Sajjan[2]

[1] Department of Chemistry, Karnatak Science College, Dharwad-580001, India

[2] Department of Chemistry, KLE Technological University, Hubballi-580 031, India

*E-mail: drrajappask@gmail.com

Received 17 February 2023; accepted 16 May 2023

Laurus Tamala leaves extract (LTLE) has been employed as a soft steel corrosion inhibitor in a 1M Hydrochloric acid media. Chemical (weight loss) and electrochemical investigations were carried out to assess the corrosion rate and percentage inhibition efficiency of the extract. The electrochemical polarization results have demonstrated that plant leaves extract functions as a mixed type inhibitor. The stability of the inhibitor is tested at elevated temperatures by weight loss method. The corrosion inhibition mechanism is interpreted through adsorption mechanism, and the LTLE components has obeyed the Langmuir adsorption isotherm for soft steel. The interaction of the components of the extract is assessed through FT-IR technique. The surface morphology, roughness and hydrophobicity in presence and absence of the extract have been characterized through SEM, AFM and water contact angle techniques respectively. The highest inhibitory efficiency is 96.21% for 24 h as recorded by weight loss method. Additionally, the DFT computations has revealed the inhibitor's adsorption through electron donor-acceptor interactions.

Keywords: Laurus Tamala leaves extract, Soft steel, Corrosion inhibitor, Tafel plots.

Metal and its alloys are fascinating industrial materials owing to their increased availability, physicochemical properties, exceptional ductility, significant mechanical characteristics, low cost, and wear resistance. These materials have been commonly applied in engineering disciplines such as casings, metal processing, seawater purification, automobiles, petroleum refineries, tube manufacturing, and gas and oil transportation. However, under the following circumstances, these materials are prone to corrode. These can be removed by proper oil well acidification, rust cleaning, acid descaling, and boiler cleansing processes performed on the equipment to protect metal components machinability and extend their service life. The corrosion processes destroy the metal surface. As a result, the mechanical characteristics of the metal are drastically diminished. During this process, metal loss from the external surface occurs. Metallic material deterioration creates severe environmental and financial issues[1-5]. Therefore, acids attacking soft steel surfaces lead to corrosion problems. Most inhibitors (organic and inorganic) are expensive, environmentally harmful, and poisonous. Inhibitors are widely used, as evidenced by their excellent anti-corrosion capacity and economic adaptability.As a result of these problems, inhibitors of plants have indeed been explored as a potential remedy[6-9]. This is due to their affordability, accessibility, low cost, inexhaustible, non-toxic, and ecological stability. Natural substances found in plants can be utilized to control or prevent the oxidation of metals and alloys in various industrial applications. Inhibitors control corrosion by blocking surface-active areas, adhering to the surface, and creating an effective barrier to corrosive ions. This has encouraged researchers to discover safe, affordable, biodegradable, and effective green corrosion inhibitors[10-12].

Furthermore, the use of green corrosion inhibitors was gained into high consideration because of their economic resilience[13-15]. Most naturally occurring phytoconstituents (plant-based) are environmentally safe and work well to prevent metal corrosion in acidic conditions. *Crotalaria Pallida-A*[16], *Dolichandra unguis-cati* [17], *Ficus tikoua* leaves extract[18], *Chamaerops humilis* leaves extract[19],

Dardagan Fruit extract[20], *Thevetia peruviana* flower extracts[21], *Portulaca grandiflora* leaf (PGL) extract[22], *Garcinia Indica* fruit extract[23], *Allium sativum* extract[24], *Garcinia livingstonei*[25], etc have been declared as suitable inhibitors in corrosive media. The chemical compounds such as alkaloids, flavonoids, saponins, terpenoids, and other chemical substances found in plant materials comprise many aromatic rings and functional groups, including heteroatoms, such as those with N, S, or O atoms. Their interaction with the metal surface can therefore demonstrate a high level of corrosion inhibition.The analysis confirms the presence of active constituents such as cinnamaldehyde, Trans-cinnamyl acetate, Ascabin[26]. Whereas the cinnamaldehyde plays an important role in the field of agriculture, medicinal field and also it is used as flavouring in foods. The trans-cinnamyl acetate used as a fragrance, a metabolite and an insecticide. The Ascabin used for fixative of solvent and essence of Musk, substitute of camphor, also used for preparation of pertussis medicine, asthma medicine, etc.The impact of Laurus Tamala leaves on living organisms has many medicinal applications such as immune response, liver and its antioxidant, anti-inflammatory, gastrointestinal tract, anticancer, antidiabetic, and antimicrobial activity[27]. Soxhlet extraction is the most often used technique for extracting analytes from solid matter. The conventional Soxhlet method has often been used in practically all analytical labs since its discovery in 1879. In addition, the Soxhlet extraction technique is still used as a reference point to assess how well the contemporary extraction process performs. The Soxhlet extraction method is extraordinarily efficient, minimizing both resources and time. Therefore, the Soxhlet extraction from Laurus Tamala leaves is the preferred technique for the proposed investigation. The Soxhlet device is schematically shown in Fig. 1. The current study was conducted to assess the effectiveness of inhibition for soft steel using the LTLE inhibitor in 1 M HCl by applying investigational and conceptual techniques.

Experimental Section

Phytochemical screening

Laurus Tamala leaves extract was subjected to a phytochemical analysis to assess phytochemical availability, including steroids, tannins, saponins, reducing sugar, phenolic compounds, flavonoids, etc. Additionally, traditional qualitative tests like $FeCl_3$, Braymer's, Shinoda's, and others were applied. The phytochemical investigation of Laurus Tamala leaf extract was conducted using the following conventional procedures.

Test for Tannins (Braymer's test)

Following the addition of 0.5 mL of the LTLE to the 3 mL of distilled water, 3-4 drops of 10% ferric chloride solution was added. If the colour of the extract turns green or blue, tannins are present. Colour changes in the final product were observed.

Test for Flavonoids (Shinoda test)

0.5 mL of LTLE extract was added to the few drops of concentrated hydrochloric acid solution along with that 2 pieces of magnesium ribbon were added. The presence of flavonoids is indicated if the extract's colour shifts to orange, pink, or purple. Colour changes in the final product were observed.

Test for Terpenoids

1 mL of acetic anhydride and 2 to 3 drops of concentrated H_2SO_4 are added to 0.5 mL of the LTLE. Terpenoids are indicated by the presence of a deep red colour. The final product's colour shift was observed.

Test for Reducing sugars (Benedict's test)

Benedict's reagent is added to 0.5 mL LTLE and boiled for 2 minutes. The extract's color changes to green, yellow or red, indicates the presence of reducing sugar. The final solution's colour shift was observed.

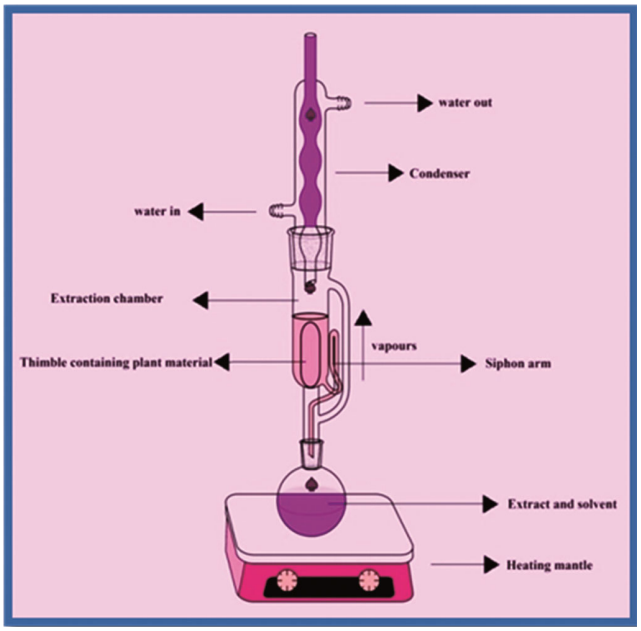

Fig. 1 — Soxhlet extraction technique

Test for Phenolic compounds

A few drops of 5% ferric chloride solution are added to 0.5 mL of the LTLE solution. The existence of the phenolic component is indicated by the appearance of dark green or bluish-black colour. The final solution's colour shift was observed.

Test for Steroids

Add 0.5 mL of the LTLE, 1 mL of $CHCl_3$, and 1 mL of concentrated H_2SO_4 from the test tube's side to the mixture. A brown ring shows that steroids are present. Colour changes in the final product were observed.

Test for Saponins

0.5 g of LTLE should be mixed with 2 mL of water (vigorously shaken). Saponins are present if there is continuous foam after 10 min. For a change in colour, the final answer was identified.

Inhibitor preparation

Laurus Tamala leaves were found at the Karnataka Agricultural University in Dharwad, India, which can be seen in Fig. 2. The leaves were gathered, cleaned with water, then kept in a hood for a week to dry. Next, the dried leaves were grounded to a fine powder. Then, soxhlet extraction was used to obtain the Laurus Tamala leaves extract using 28 g of LTLE powder with 280 mL of ethanol. The remains solvent in the extract was retrieved through the rotary evaporator then the extract was utilized for stock solution preparation which was employed for the tests with a concentration range of 20, 40, 60, and 80 ppm.

Electrolyte preparation

To prepare the 1 M HCl solution, AR-grade hydrochloric acid was diluted with double-distilled water, which was used as an electrolyte and a corrosive medium. Various concentrations of LTLE solutions prepared in 1 M HCl solution were utilized for the tests.

Fig. 2 — Laurus Tamala leaves

Specimen preparation

Soft steel specimen (having the following percentage composition: Mn = 0.29, C = 0.11, P= 0.08, Si = 0.05, S = 0.02, Ni = 0.01, Cu = 0.01 and remains Fe) of dimension 5cm x 1cm x 0.1 cm (l × b × h) were treated with dilute HCl solution to remove the upper coating and then, polished with an emery paper of 180, 400, 1000, 1500 and 2000 grade and washed with double distilled water then dried and the specimens were kept in desiccators. The pre-treated samples were used for further experimental studies.

Weight loss technique

The soft steel weight-loss research was done to determine the LTLE corrosion inhibition in 1 M HCl. Pre-treated coupons were weighed and dipped in varying LTLE concentrations of 1 M HCl. After completing the test, before being weighed, coupons were cleansed, dehumidified, weighed, and stored in a desiccator. The average weight loss results were recorded using the same methodology.

Electrochemical measurements

Using the CH-Electrochemical instrument type CH1660E, electrochemical techniques such as potentiodynamic polarisation and EIS were investigated. For electrochemical measurements, a three-electrode cell assembly was used. It consisted of a saturated calomel electrode serving as the reference electrode (RE), a platinum electrode serving as the counter electrode (CE), and a soft steel coupon with an exposed area of 1 cm^2 that was mounted in a specimen holder as the working electrode (WE). The soft steel was submerged in the experimental solution for 40 min to stabilize the open circuit potential. The OCP polarisation curves were produced using a 200 mV potential range and a scan rate of 1 mV s^{-1}. The Nyquist plots were obtained at an amplitude of 5 mV s^{-1}, 0.1 Hz to 100 kHz frequency range. The relevant circuit is fit by Z-simp 3.21 based on Nyquist impedance values.

Thermodynamic and adsorption isotherm considerations

The component of Laurus Tamala leaves extract's adsorption on the metal substrate determines its performance in corrosion protection. The adsorption kinetics was assessed at the temperature range from 300 to 330 ±1K for 1 M HCl. Employing

conventional approaches, the thermodynamic evaluation of the adsorption kinetics and fitting of the data into an appropriate model for the adsorption isotherm. In this experiment, the LTLE bonded to the Langmuir adsorption isotherm and further calculated and discussed the various thermodynamic parameters.

FT-IR spectrum

Using a Nicolet 5700 FT-IR spectroscope, the FT-IR spectra of crude LTLE and their interaction with the soft steel surface in 1 M HCl were obtained.

Surface studies

Scanning electron microscopy (SEM) and atomic force microscopy (AFM) methodologies were used to assess soft steel surface morphology. Water contact angle analysis was considered to know the hydrophobic nature of the specimen surface.

DFT calculations

Quantum chemical computations were done using Materials Studio 8.0, applying the DMol^3 module based on density functional theory (DFT) (Accelrys Company). First, the optimized geometry of the three Laurus Tamala leaves inhibitor molecules was optimized using the generalized gradient using the BLYP (GGA/BLYP) technique approximations (GGA). The optimization was followed by a quantum chemical calculation using the same technique.

Results and Discussion

Phytochemical screening

The results of phytoconstituents in LTLE are shown in Table 1. There are phenolic substances, tannins, flavonoids, reducing sugars, and terpenoids contained in the extract. These components predominantly have strong inhibitory properties. The components of LTLE create an adsorption layer that protects the soft steel against corrosion. Due to the biological species in theLTLE extract adhering to the soft steel surface, decreasing the area vulnerable to corrosion, the corrosion rate on soft steel can be reduced [28,29].

Table 1 — Phytochemicals present inLaurus Tamala leaves extract

Sl. No.	Compounds	Tests	Results
1.	Tannins	Braymer's test	++
2.	Flavonoids	Shinoda test	++
3.	Terpenoids	Acetic anhydride + Conc. H_2SO_4 test	++
4.	Reducing sugar	Benedicts reagent	++
5.	Phenolic compound	5% $Fecl_3$ solution	++
6.	Steroids	Salkowaski's test	--
7.	Saponins	Foam test	--

Weight loss measurements

Following investigations on weight loss were performed on soft steel samples submerged in 1 M HCl solution with and without varying strengths of LTLE at 300±1K. The specimen's rate of corrosion, surface coverage (θ), and performance of inhibition ($\%\eta_w$) were determined using Eqs 1, 2, and 3.

$$v = \frac{534W}{ATD} \quad \ldots (1)$$

Where v = rate of corrosion of soft steel (mpy), W = weight loss (mg), A = area of soft steel (in square inches), D = density of soft steel, and T = immersion time (in h).

$$\theta = \frac{W_1 - W_2}{W_1} \quad \ldots (2)$$

Accordingly, W_1 denotes the weight reduction of soft steel strips without LTLE and W_2 indicates the weight reduction with LTLE.

$$\%\eta_W = \frac{W_1 - W_2}{W_1} \times 100 \quad \ldots (3)$$

where W_1 and W_2 represent the weight reduction of the soft steel strips with and without LTLE, respectively

Table 2 shows the corrosion rate for different LTLE inhibitor concentrations for soft steel and illustrates the percentage inhibition efficiency ($\%\eta_W$) from 1, 2, 3, 4, 6, and 12 h at 300±K. The results in Table 2 show that when the concentration of the inhibitor increases, the corrosion rate value decreases, and the inhibition efficacy increases. The primary cause of this is the LTLE inhibitor's components adhering to the surface of the soft steel, forming a thick coating that slows corrosion. This study demonstrates that the frequent interaction of LTLE improved with higher LTLE concentration in 1 M HCl. The highest $\%\eta_W$ of 96.21 was attained for an hour at an ideal 80 ppm LTLE inhibitor concentration. More than 80 ppm of LTLE can reduce interactions between metals and the inhibitor, causing the inhibitor to be replaced by H_2O or chloride ions and reducing the inhibitor's efficacy. Acidic liquids also encourage the evolution of hydrogen.

As a consequence, on the surface of the metal, the mass does not accumulate. In the acid media, the LTLE components go through protonation, which slows down the reduction process. The presence of LTLE components reduces soft steel corrosion because they adhere to the metallic surface and act as a barrier to protect it from acidic conditions [30-32].

Polarization studies

Electrochemical polarization measurement is an essential technique for calculating the parameters of corrosion kinetics, such as cathodic and anodic reactions during the process of corrosion. The potentiodynamic polarization method demonstrated was used to examine the behaviour of soft steel in 1 M HCl with and without the LTLE in Fig. 3. The study helps to comprehend the relationship between current and potential with and without an LTLE inhibitor in a 1 M HCl solution for soft steel corrosion. Table 3 displays the calculated corrosion rate (υ) in mpy, the anodic Tafel slope (β_a), the cathodic Tafel slope (β_c), the corrosion current density (i_{corr}), the corrosion potential (E_{corr}), and the percentage inhibition efficiency ($\%\eta_w$). For soft steel in 1 M HCl, the inhibitory performance of LTLE was calculated using Eq. 4.

$$\%\eta_w = \frac{i^o_{corr} - i_{corr}}{i^o_{corr}} \times 100 \quad \ldots (4)$$

Where, the corrosion current densities in the blank and with the LTLE inhibitor, respectively, are represented by the variables i^0_{corr} and i_{corr}. The LTLE inhibitor addition caused a significant change in the polarization curves by reducing the corrosion current density, suggesting that LTLE controlled the soft steel corrosion in a corrosive medium [33]. The LTLE caused the equilibrium corrosion potential (E_{corr}) to shift to greater negative values, indicating that LTLE makes the corrosion process more complex. Corrosion current density without (i^o_{corr}) and with (i_{corr}) measurements were used to estimate the

Table 2 — Weight loss outcomes for various inhibitor concentrations on soft steel in 1M HCl at 300±1K

Time (h)	Conc. (ppm)	Corrosion rate (mpy)	Inhibition efficiency ($\%\eta_W$)	Surface coverage (θ)
1	Blank	183.85		
	20	36.77	80.00	0.8000
	40	24.51	86.66	0.8666
	60	18.39	90.00	0.9000
	80	12.26	93.33	0.9333
2	Blank	174.66		
	20	21.45	87.71	0.8771
	40	18.39	89.47	0.8947
	60	15.32	91.22	0.9122
	80	12.25	92.98	0.9298
4	Blank	163.94		
	20	13.79	83.92	0.8392
	40	12.26	92.52	0.9252
	60	9.19	89.28	0.8928
	80	7.66	91.07	0.9107
5	Blank	212.04		
	20	18.39	91.32	0.9132
	40	15.93	92.48	0.9248
	60	14.71	93.06	0.9306
	80	13.48	93.64	0.9364
6	Blank	310.51		
	20	16.34	94.73	0.9473
	40	15.32	95.06	0.9506
	60	20.43	93.42	0.9342
	80	18.39	94.07	0.9407
12	Blank	305.40		
	4.5	19.41	93.64	0.9364
	6.0	18.90	93.81	0.9381
	7.5	17.36	94.31	0.9431
	9.0	16.85	94.48	0.9448
24	Blank	236.20		
	20	13.02	94.48	0.9448
	40	12.26	94.81	0.9481
	60	9.19	96.10	0.9610
	80	8.94	96.21	0.9621

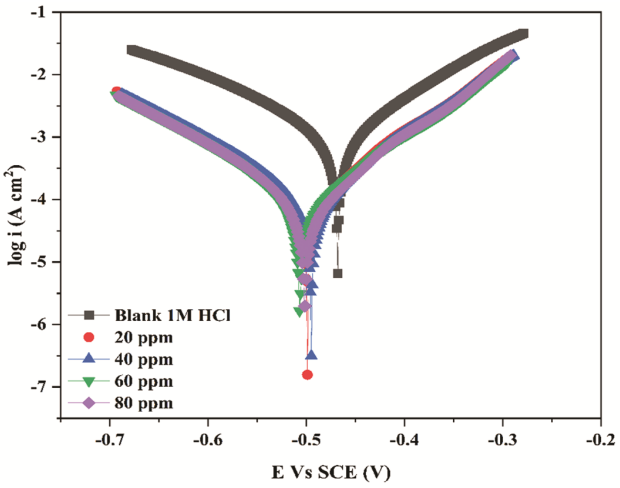

Fig. 3 — Soft steel polarization curve in the presence and absence of LTLE at various concentrations after being dipped in 1M HCl

Table 3 — Outcomes of polarization experiments in 1 M HCl with and without LTLE

Conc. of acid (M)	Conc. (ppm)	E_{corr} (V vs SCE)	I_{corr} (A cm^{-2})	β_a (V/dec)	$-\beta_c$ (V/dec)	C.R. (mil/yr)	$\%\eta_w$
1 M HCl	Blank	-0.468	1.043×10^{-3}	9.847	7.673	4.774×10^{2}	
	20	-0.499	1.058×10^{-4}	10.992	8.923	4.842×10^{1}	89.85
	40	-0.495	9.660×10^{-5}	11.027	9.011	4.422×10^{1}	90.73
	60	-0.507	8.753×10^{-5}	11.197	9.166	4.007×10^{1}	91.60
	80	-0.502	8.085×10^{-5}	11.780	9.118	3.701×10^{1}	92.24

inhibitory efficacy for soft steel in the presence and absence of various concentrations of LTLE in 1 M HCl. As the inhibitor concentration rise, i_{corr} value was significantly reduced, and the percentage inhibition efficiency $(\%\eta_w)$ enhanced. This reduction in corrosion current density results from the molecules of inhibitor interacting with the soft steel surface, acting as a barrier of protection and reducing active sites, confirming the soft steel surface's ability to bind LTLE [34].

According to the electrochemical polarization experiment results, in a 1 M HCl solution, LTLE is a superior anticorrosive agent for soft steel. If the E_{corr} is more than ±85 mV, the inhibitor can be categorised as either cathodic or anodic, but in present studies, the obtained E_{corr} values were 39 mV, from which we can confer that LTLE functions as a mixed type. Polarization techniques obtained a maximum of 92.24 $\%\eta_w$ for 1 M HCl. The fact that (β_a) and (β_c) values significantly changed as the inhibitor concentration surged implies that LTLE adsorption on the soft steel lessens soft steel corrosion in acid solution. Blocking the binding sites on soft steel significantly reduces the cathodic reaction, which is accompanied by a hydrogen evolution reaction [35].

EIS studies

The impedance Nyquist plots for soft steel in 1 M HCl, both with and without different LTLE concentrations, are shown in Fig. 4. The size of the semicircles is associated with the change in surface roughness, inhomogeneity, and inhibitor adsorption[36].

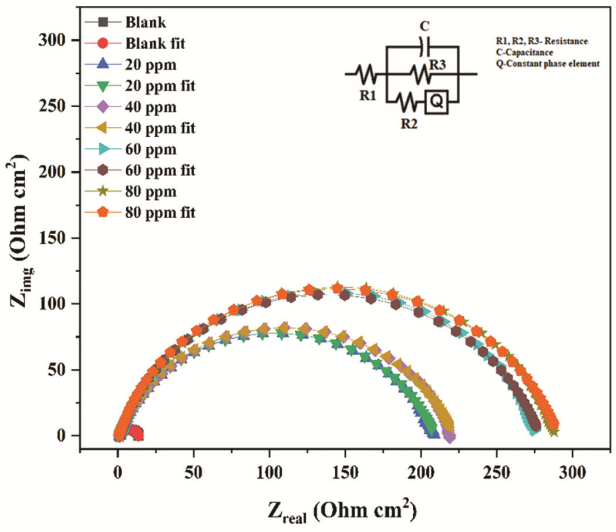

Fig. 4 — Soft steel Nyquist plots in 1 M HCl, both with and without LTLE at various concentrations

The semicircle's diameter will significantly rise in proportion to the charge transfer resistance. Adding LTLE to the acidic media improved the semicircle's diameter compared to the blank. It exhibited further improvement in the diameter of the semicircle when the LTLE concentration was raised. This proved that LTLE resists soft steel dissolution and forms a protective layer on its surface. Nyquist semicircles exhibit a single capacitive loop in LTLE inhibitor solution that is both inhibited and uninhibited, suggesting that LTLE regulates the corrosion reaction through anodic metal dissolution through a single charge transfer process[37]. A five-element equivalent circuit, R_1, R_2, R_3, Q, (the constant phase element), and C as the Capacitance, was proposed using Z_{simp}Win software 3.21. The experimental data from the EIS investigation was well matched to a similar circuit model, as represented in Fig. 4. As seen in Fig. 4, the experimental curve obtained fits the predicted curve for an optimal inhibitor concentration of 80 ppm. Table 4 lists the calculated resistance double-layer capacitance (C_{dl}), polarization (R_p), chi-squared, and percentage inhibition efficiency $(\%\eta_w)$. The double-layer capacitance and inhibitory efficiency were calculated using Eqs 5 and 6.

$$C_{dl} = (QR_{ct}^{1-n})^{1/n} \quad \ldots (5)$$

$$\%\eta_w = \frac{R_{ct} - R_{ct,0}}{R_{ct}} \times 100 \quad \ldots (6)$$

Where the charge transfer resistances with and without LTLE are shown, respectively, by R_{ct} and $R_{ct,0}$. However, when the amount of LTLE inhibitor was raised in 1 M HCl, both R_p and inhibitory efficiency values increased significantly, showing that LTLE has been blocked the reactive sites of the soft steel surface[38]. According to the estimated outcomes, it is clear that the inclusion of LTLE increased $R_p$values while decreasing C_{dl} values. The increase in resistance polarization with the adsorption mechanism, which replaces water molecules on the metal surface covered with the

Table 4 — Data from EIS analysis for soft steel in the presence and absence of LTLE in 1M HCl

Concentration *(ppm)*	R_{ct} *(Ω cm²)*	C_{dl} *(μF/cm²)*	$(\%\eta_w)$	Surface coverage *(θ)*
Blank	19.31	42.17	-	-
20	213.04	26.96	90.94	0.9094
40	224.81	25.65	91.41	0.9141
60	283.61	24.41	93.19	0.9319
80	297.46	23.68	93.51	0.9351

inhibitor, causes an increase in the concentration of the inhibitor, making the charge transfer process more complex[39]. A drop in the local dielectric constant or an increase in the thickness of the electrical double layer might affect the inhibitors adsorption at the metal/solution interface. It is confirmed by the fact that C_{dl} drops as LTLE concentration rises. The polarization experiment outcomes strongly agree with the $\%\eta_w$ calculated utilizing the impedance spectroscopy technique. The inhibitors performance in lowering the corrosion rate is correlated with the high stability and hydrophobicity of the outer inhibitor layer over the metal surface[40].

Activation parameters

Table 5 represented the efficiency of LTLE's inhibition lowers from 300 to 330 ±1K in 1 M HCl. With every 10K increase in temperature, the metal loses its strength from 300 to 330±1K. Reduced $\%\eta_w$ with rising temperature implies that the protective coating cannot withstand longer contact times. The increased concentration of LTLE improves the $\%\eta_w$ and lowers the soft steel corrosion rate, as seen in Table 5. Adsorption of LTLE develops an adhered layer on the surface of the soft steel[41]. By examining the differences in the corrosion rate of soft steel when exposed to various solution temperatures, this experiment shows the activation energy (E_a^*) involved with the corrosion process[42]. The activation energy (E_a^*) is calculated using the Arrhenius Eq. 7.

$$lnv_{corr} = lnA - \frac{E_a^*}{RT}, \quad \ldots (7)$$

Where the abbreviations A stands for the Arrhenius pre-exponential factor, R for the gas constant, T for temperature, and E_a^* for apparent activation energy. E_a^* values were calculated from the slope (-E_a^*/R) of the graph's straight lines, which are shown in Table 5, and the Arrhenius plot was created using lnv_{corr} vs 1000/T (Fig. 5). The presence of inhibitors prevents the dissolution of metal, as shown by the higher E_a^* values in the presence of inhibitors compared to in the absence of inhibitors. The higher Ea^* value in the presence of an inhibitor molecule is also responsible for the increase in inhibitor adsorption, which results in the creation of mass and charge transfer barriers. The standard activation enthalpy and standard activation entropy, abbreviated as H^* and S^*, have been calculated using the transition state equation and are represented as

$$ln\frac{v_{corr}}{T} = \left[ln\frac{R}{Nh} + \frac{\Delta S^*}{R}\right] - \frac{\Delta H^*}{RT}, \quad \ldots (8)$$

where N = Avogadro's number and h = Plank's constant.

Fig. 6 shows the correlation between $ln\ (v_{corr}/T)$ against $1000/T$, which gave a slope of -ΔH^*/R and an intercept of ΔS^*=intercept-ln(R/Nh). The variables obtained, such as enthalpy and entropy, are listed in Table 6. Positive ΔH^* values indicate more significant inhibitor adsorption on the soft steel surface and

Table 5 — Effect of temperature on soft-cast steel in 1M HCl at varying LTLE concentrations with a 1-h immersion time in 1M HCl for 300±1K - 330±1K

Temp. *(K)*	Concentration *(ppm)*	Corrosion rate *(mpy)*	Percentage inhibition efficiency *($\%\eta_w$)*	Surface coverage *(θ)*
300	Blank	189.98		
	20	24.51	87.10	0.8710
	40	18.38	90.32	0.9032
	60	12.26	93.55	0.9355
	80	6.13	96.77	0.9677
310	Blank	465.76		
	20	79.67	82.89	0.8289
	40	67.41	85.52	0.8552
	60	55.16	88.16	0.8816
	80	36.77	92.11	0.9211
320	Blank	723.15		
	20	159.34	77.97	0.7797
	40	134.83	81.35	0.8135
	60	110.31	84.74	0.8474
	80	91.93	87.28	0.8728
330	Blank	1060.22		
	20	281.91	73.41	0.7341
	40	245.14	76.88	0.7688
	60	202.24	80.92	0.8092
	80	165.47	84.39	0.8439

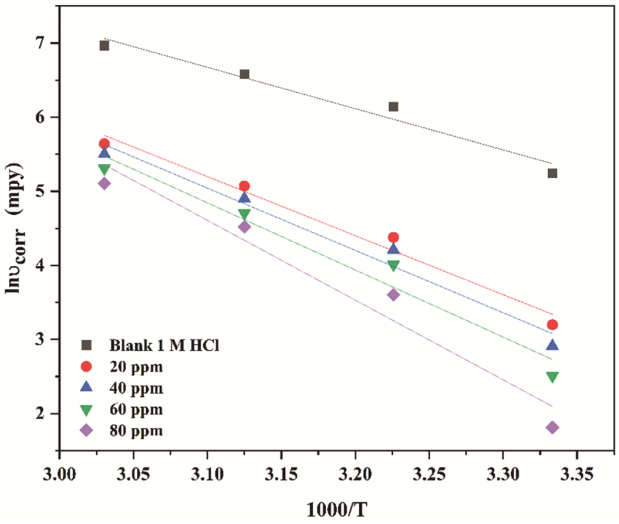

Fig. 5 — Arrhenius plots for soft steel with and without LTLE

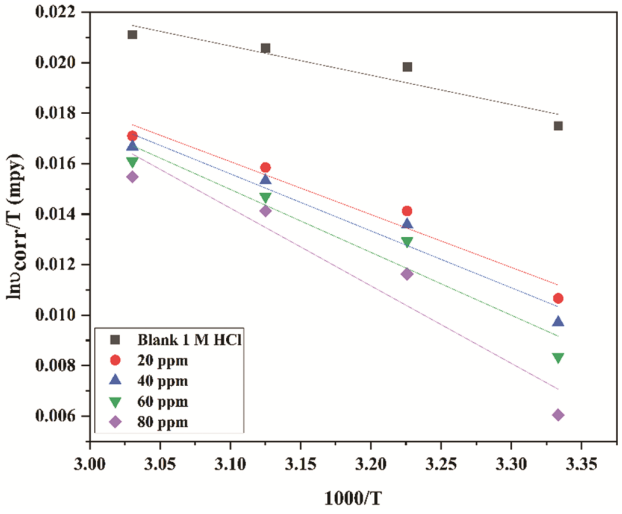

Fig. 6 — Arrhenius transition plots for soft steel

Table 6 — Activation parameters for soft steel in1 M HCl with and without LTLE

Conc. *(ppm)*	*Ea** *(kJ mol^{-1})*	*A* *(kJ mol^{-1})*	*ΔH** *(kJ mol^{-1})*	*ΔS** *(J mol^{-1} K^{-1})*
Blank	46.32	2.503×10^{10}	96.53	-23.703
20	66.30	9.854×10^{12}	174.10	-23.679
40	70	3.357×10^{13}	187.65	-23.674
60	75.35	2.020×10^{14}	207.02	-23.668
80	89.50	3.118×10^{16}	255.66	-23.650

possess a rise in endothermic nature. The LTLE components adsorption on soft steel surfaces prevents the active sites from functioning, interfering with hydrogen ion interactions. In the rate-determining phase, the (*Δ*S*) activation entropy factors are increased by the presence of LTLE, which reduces disorder from the activated complex to the reactants[43-46].

Calculations of adsorption isotherm

Investigating the soft steel adsorption mechanism on the external surface provides helpful information about the corrosion inhibition mechanism. LTLE may adsorb on the metal surface by physical adsorption, chemical adsorption, or both, depending on several factors like the electrolyte, the type of the metal, and the temperature of the solution. The inhibition performance achieved by the weight loss method was used to determine surface coverage. By plotting C_{inh}/θ ppm vs. C_{inh} ppm, it is evident that the LTLE extract's components adhere to the Langmuir adsorption theory (Fig. 7). The standard Eq. 9 was used to assess the adsorption process in this model.

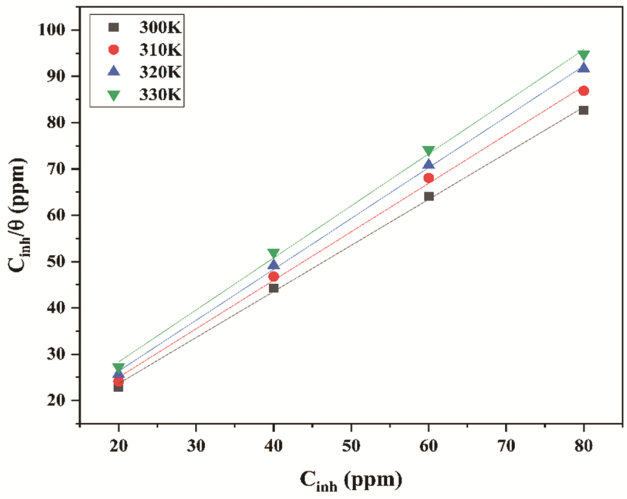

Fig. 7 — Plot of Langmuir adsorption isotherm for varying LTLE inhibitor concentrations

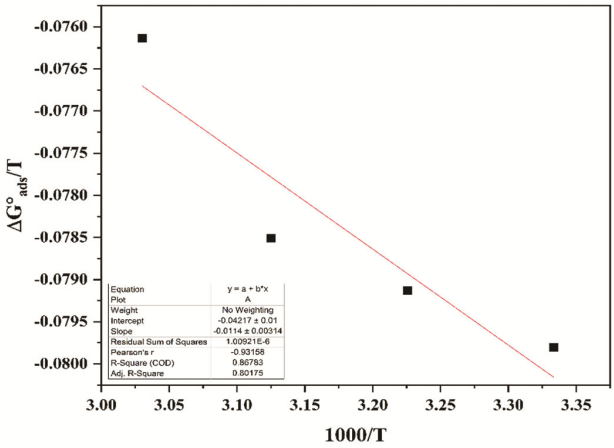

Fig. 8 — Graph of ΔG^o_{ads}/T vs. 1000/T for 1 M HCl

$$\frac{C}{\theta} = \frac{1}{K_{ads}} + C \qquad \ldots (9)$$

In the above equation, C signifies the concentration of LTLE, θ signifies surface area coverage, and K_{ads} signifies the process of adsorption equilibrium constant. The values of K_{ads} were attained utilizing the intercepts of C_{inh}/θ axis[47]. Adsorption free energy (ΔG^o_{ads}) are typically utilized to analyze the interactions between the soft steel surface and LTLE constituents. The equilibrium constant for the adsorption process is K_{ads}, which is associated to ΔG^o_{ads} by the given equation 10.

$$\Delta G^o_{ads} = -2.303RTlog\left(K_{ads} \times C_{H_2O}\right), \qquad \ldots (10)$$

Where R is the gas constant, T is the temperature, and C_{H_2O} equals 1000 g/L of concentration of water. As seen in Fig. 8, the slope values of ΔG^o_{ads}/T vs. *1000/T*

graph was utilized to quantify the adsorption enthalpy (ΔH^o_{ads}). The adsorption entropy (ΔS^o_{ads}) is determined by using the Gibbs Helmholtz Eq. 11.

$$\Delta S^o_{ads} = \frac{(\Delta H^o_{ads} - \Delta G^o_{ads})}{T}, \quad \ldots (11)$$

The parameters K_{ads}, ΔG^o_{ads}, ΔH^o_{ads}, and ΔS^o_{ads} are mentioned in Table 7. Greater K_{ads} values in the table demonstrate good LTLE inhibitor inhibition performance and electrostatic contact between the double layer on the interface between two phases and the components adsorbed, as shown in Table 7. Thermal agitation of LTLE components is caused by increased temperature, lowering LTLE molecules adsorbed to the metallic surface and facilitating their interchange with the solution. The reduced (negative) ΔG^o_{ads} values are attributed to the spontaneous adsorption and protective coating formed on the surface of the soft steel.

The data of ΔG^o_{ads} near -20 kJ/mol imply physisorption, and values near -40 kJ/mol imply chemical adsorption. The values of ΔG^o_{ads} calculated using the conventional approach for 1 M HCl that ranges from -23.941to -25.125 kJ/mol. The findings imply that interactions between physical and chemical processes are crucial to the adsorption of LTLE elements on the soft steel surface[48]. The ΔH^o_{ads}(-11.40 kJ/mol) negative data demonstrate that the LTLE adsorption process is exothermic. Positive values of ΔS^o_{ads} strongly suggest an increase in disorder due to the LTLE molecules adsorbed on the soft steel surface through the desorption of H_2O molecules, leading to a rise in adsorption entropy[49].

FTIR studies

The phytochemical screening tests reported many phytochemical components, such as tannins, flavonoids, terpenoids, reducing sugars, and phenolic compounds. According to DFT studies, it has been identified that Cinnamaldehyde, Trans-cinnamyl acetate, and Ascabin are the primary components included in the LTLE (Fig. 9) These significant components, which comprise the functional groups, are confirmed in the FT-IR analysis as seen in Fig. 9a and 9b**.** These groups of the LTLE may interact on the surface of the specimen and inhibit soft steel corrosion. The inhibition mechanism in this instance was probably brought about by the LTLE component's adherence to the soft steel surface and the formation of a thin, protective coating on its surface of it.

Table 7 — Data on the thermodynamics of LTLE adsorption on soft steel at various temperatures in 1 M HCl

Temp. (K)	K_{ads}	ΔG^0_{ads} (kJ mol^{-1})	ΔH^0_{ads} (kJ mol^{-1})	ΔS^0_{ads} (J mol^{-1} K^{-1})
300	265.22	-23.941	-11.40	41.80
310	244.60	-24.530	-11.40	42.35
320	226.94	-25.122	-11.40	42.88
330	170.65	-25.125	-11.40	41.59

The FTIR spectra for the pure LaurusTamala leaves extract are shown in Fig. 9a shows a significant band of the –OH stretching at 3455 cm^{-1}. At 1654 cm^{-1}, the C=C stretching is visible, while at 1439 cm^{-1} is where the CH_2 bending is visible. At 1112 cm^{-1}, it is possible to see C-O stretching. The FTIR spectra of the soft steel specimen after treatment with the selected inhibitor (LTLE) containing 1 M HCl are shown in Fig. 9b. These spectra show a significant difference in the absorbance peaks of the functional groups concerning pure Laurus Tamala extract. The bandwidth at 3434 cm^{-1} proves that the -OH group is extending. The C=C stretching frequency, 1636 cm-1, is slightly different from the pure extract. Peaks that emerge at 1430 cm^{-1} and 1059 cm$^{-1,}$ respectively, indicate CH_2 bending and C-O stretching. These results imply that functional groups are present in the LTLE extraction, enabling the extract to function as a corrosion inhibitor. The oxygen (heteroatom) and pi bond make adsorption on soft steel simple. In addition, electron-rich entities may quickly form thick layers on substrate surfaces due to their extreme affinity for electrons.

Scanning electron microscope

The scanning electron microscope images demonstrate the morphological characteristics of the adherent coating formed on the coupons immersed in

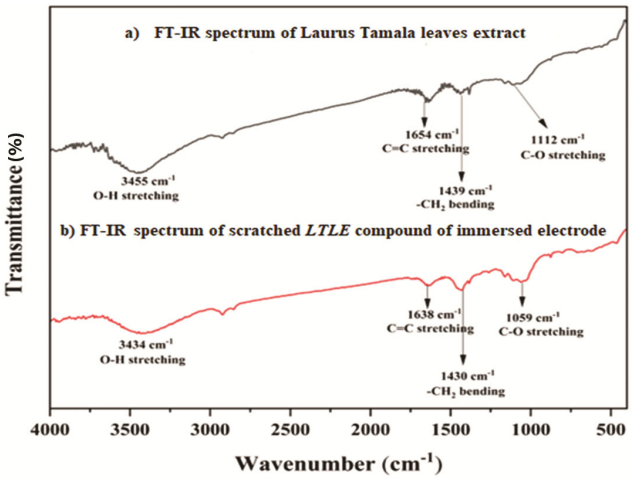

Fig. 9 — FTIR spectra of (a) Pure LTLE and (b) In the presence of LTLE and 1M HCl, scratched compound was collected from the soft steel surface

the acidic media for 24 hours in the presence of the optimal LTLE concentration. The SEM images of the bare specimen, soft steel dipped in 1M HCl without LTLE and with LTLE inhibitor, are shown in Fig. 10. The SEM image of the bare specimen shows that the surface appears clean and smooth, as seen in Fig.10a. In contrast, the soft steel dipped in 1M HCl for 24 h, the surface is severely damaged by the acid attack and has many cracks and cavities on its surface, as depicted in Fig.10b. A SEM micrograph recorded during LTLE's presence at 80 ppm, the surface of the soft steel is much better homogeneous and exhibits less external damage to the surface, as seen in Fig.10c. In addition, it shows that LTLE prevents corrosion by producing a protective layer around the external surface of the test coupon. The SEM micrographs obtained here confirm the findings of weight loss and electrochemical techniques[50-52].

AFM analysis

Atomic force microscopy is a helpful tool for determining morphological characteristics at the nano- to micro-scale and has recently emerged as a new methodology for evaluating the influence of corrosion inhibitors on metals. AFM study helps to estimate the average roughness *(R_a)* intended to assess the inhibitor's action on the surface of the soft steel. Based on R_a values, the adsorption mode on soft steel may be explained in detail. Fig. 11 shows three-dimensional images of soft polished steel and soft steel with and without LTLE in 1 M HCl, and the calculated parameters are presented in Table 8. The average roughness obtained values from bare (polished), corroded, and inhibited specimens indicate the adsorption of LTLE on the soft steel surface. Thus, according to Table 8, the average roughness of abraded soft steel is 30.189 nm and that of soft steel dipped in 1 M HCl for 3 hours without LTLE is 276.99 nm. The $R_a$value of soft steel immersed in 1 M HCl with 80 ppm LTLE was 73.274 nm, nearer to the bare soft steel. AFM results indicate that LTLE binds to the soft steel surface, reducing the corrosion rate[53, 54].

Contact angle tests

Water contact angle (WCA) research offers further details on procedures like wetting, absorption, and the

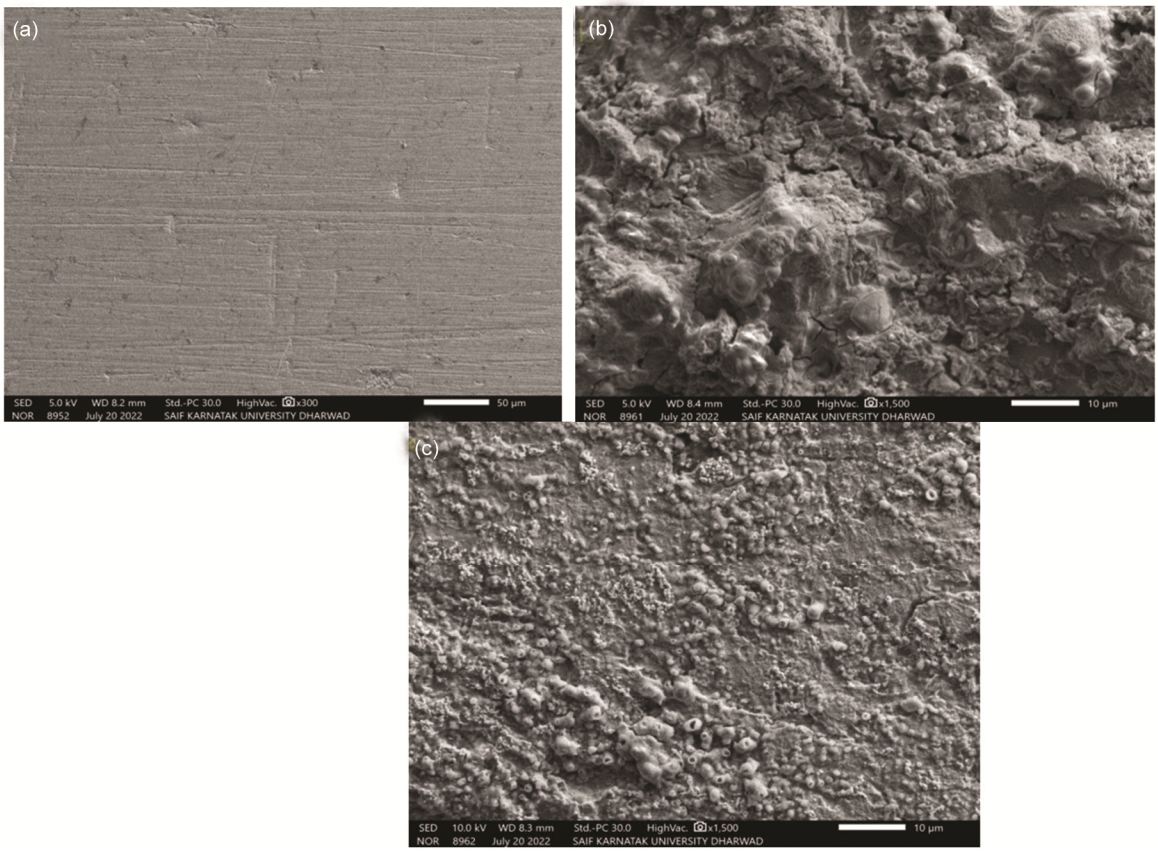

Fig. 10 — SEM analysis of soft steel: (a)= polished surface of soft steel; (b)= Soft steel submerged in 1 M HCl for 24 h; (c)= Soft steel dipped for 24 h in 1 M HCl with 80 ppm of the LTLE

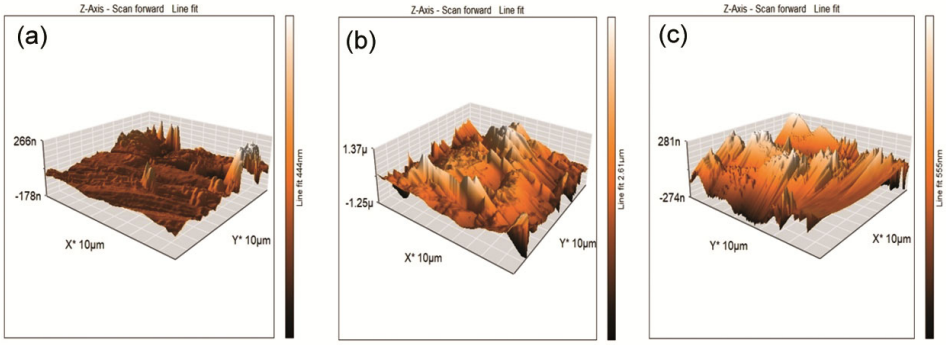

Fig. 11 — 3D AFM micrographs: (a) signifies a polished soft steel surface; (b) soft steel submerged for 3 h in 1 M HCl; (c) soft steel surface in 1 M HCl bearing 80 ppm of LTLE

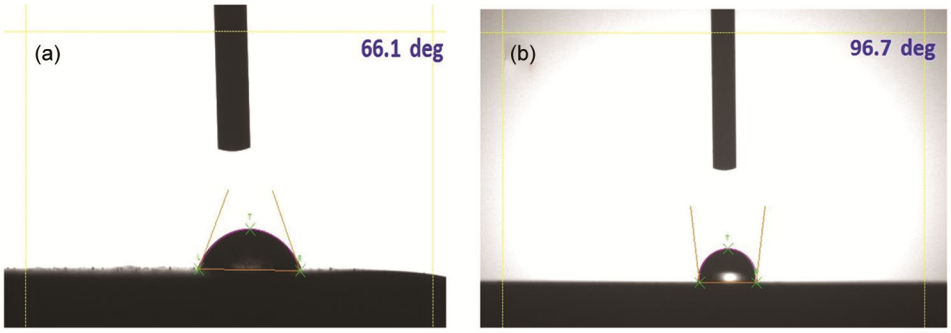

Fig. 12 — Contact angle studies: (a) = Soft steel submerged in 1 M HCl (66.1° contact angle); (b)= Soft steel dipped in 1 M HCl with 80 ppm of LTLE (96.7° contact angle)

Table 8 — LTLE AFM results

Specimen	Conc. (ppm)	Average roughness (Sa) (nm)	Root mean square roughness (Sq) (nm)
Polished soft steel	-	30.189	49.429
Blank 1 M HCl	-	276.99	343.39
LTLE	80	73.274	96.793

surface adhesion of the metal. In this study, WCA measurements give insights into the hydrophilicity/ hydrophobicity of the uninhibited and inhibited soft steel surface. The action of the contact angle has been found after adding the LTLE inhibitor to 1M HCl. The contact angle of lesser values of the uninhibited sample is responsible for forming hydrogen bonds between antagonistic acidic molecules and metal oxides, as seen in Fig. 12a, with a contact angle value of 66.1°. In addition, the contact angle results show that the corrosion product and surface heterogeneity developed on the metal surface impact the contact angle criteria.

Furthermore, adding 80 ppm of LTLE inhibitor to 1M HCl increases the contact angle values, improving the metal substrate's hydrophobicity, as shown in Fig. 12b, with a contact angle of 96.7°. The higher the amount of LTLE in the acidic medium, higher is the contact angle, suggesting the formation of hydrogen bonds of decreased ability between the metal and solution interface. The research has revealed that the presence of LTLE prevents the creation of hydrogen bonds and increases the metallic surface's hydrophobicity owing to a lack of water, which reduces the corrosion of soft steel metal[55].

Quantum chemical calculation

The complex mechanisms and relationship between the chemical interactions of CTLE molecular orbitals with the atomic orbitals of iron have been extensively studied using quantum chemical approaches, which have been widely applied[56–58]. Using the level of density functional theory (DFT) developed by (Accelrys Company) level, the optimized geometrical shapes, ground state molecular orbital energies (HOMO, LUMO), and border molecular orbitals of the investigated active phytochemicals are depicted in Fig. 13. The electrostatic potential map in Fig. 13 also sheds light on the general electrostatic impact the molecule created at the site of charge dispersion of the active component from LTLE[59]. The DFT method revealed the electronic characteristics (E_{HOMO}, E_{LUMO}, and Dipole moment). Other quantum chemical

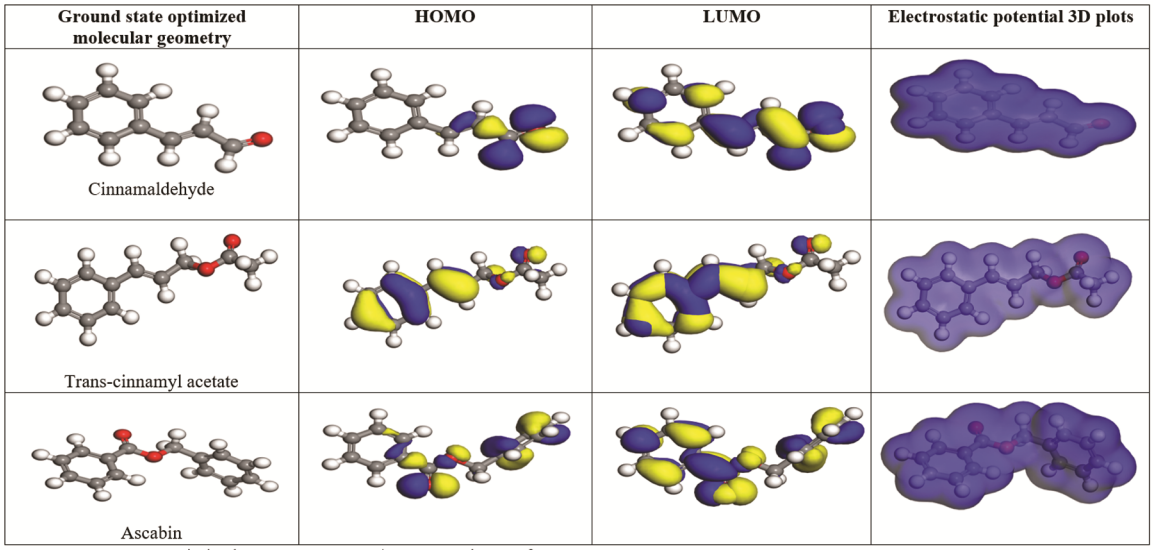

Fig. 13 — Optimized geometry, HOMO/LUMO, and ESP of LTLE

Table 9 — Computational results of an orbital value obtained of the five LTLE corrosion inhibitor molecules

Molecule	E_{HOMO} (eV)	E_{LUMO} (eV)	ΔE (eV)	I	A	χ	α	η	S	ω	ΔN
Cinnamaldehyde	-5.7449	-3.2323	2.513	5.745	3.232	4.4886	-4.4885	1.2563	0.6281	8.0185	0.9996
Trans-cinnamyl acetate	-5.7465	-2.1972	3.5492	5.746	2.197	3.9715	-3.9715	1.7745	0.8873	4.4443	0.8533
Ascabin	-6.2439	-2.3254	3.9185	6.244	2.325	4.2845	-4.2845	1.9595	0.9798	4.6841	0.6929

parameters, such as the energy gap (ΔE), chemical hardness (η), chemical softness (S), electrophilicity index (ω), absolute electronegativity (χ), and electron transfer from the extracted molecule to the metal surface (ΔN), were evaluated using the Eqs 12 to 17.

$$\Delta E = E_{LUMO} - E_{HOMO} \quad \ldots (12)$$

$$\chi = \left(\frac{IP+EA}{2}\right) \quad \ldots (13)$$

$$\eta = \left(\frac{IP-EA}{2}\right) \quad \ldots (14)$$

$$S = \frac{1}{2\eta} \quad \ldots (15)$$

$$\omega = \frac{\mu^2}{2\eta} \quad \ldots (16)$$

$$\Delta N = \frac{X_{metal} - X_{inh}}{2\,(\eta_{metal} + \eta_{inh})} \quad \ldots (17)$$

With a more significant value indicating a molecule's capacity to donate electrons to the correct acceptor unoccupied d orbitals of the soft steel Fe atoms, the E_{HOMO} is referred to as an electron donor. The unfilled 3D orbitals might interact with the HOMO of the inhibitors. Additionally, a full 4s orbital might give electrons to the LTLE's LUMO, as E_{LUMO} frequently gauges molecules' tendency to take electrons. Therefore, the likelihood of the molecules receiving electrons increases with decreasing E_{LUMO} values[60]. According to the information in Table 9, the molecules' strong stability is shown by the high energy gap between E_{HOMO} and E_{LUMO}.

Furthermore, a smaller energy gap makes polarizing the molecule easier[61]. A higher electronegativity value (χ) indicates a more extraordinary ability to gain electrons since it assesses a molecule's capability to attract electrons[62]. The higher the chemical hardness (η) value, the more excellent the charge transfer resistance of the molecule. According to reports in the literature[63], the LTLE inhibitor is supposed to donate an electron to the soft steel surface if ΔN is less than 3.6. Since ΔN (0.6929 to 0.9996) is less than 3.6, it is proved that LTLE interacts significantly with the surface of the metal in this experiment. To compute the ratio of electrons transferred as per Lukovits, (ΔN) should be less than 3.6; this demonstrates the soft steel surface's ability to transfer electrons[64-66].

Conclusion

With the use of experimental and theoretical methods, the Laurus Tamala leaves extract was proven to be a potential corrosion inhibitor for the

protection of soft steel in 1M HCl solution. LTLE efficaciously decreases soft steel corrosion rate in 1M HCl, where the $\%\eta_w$ rises with a higher inhibitor concentration of 80 ppm with a maximum of 96.21for weight loss measurements. The LTLE extract functioned as a mix-type inhibitor and decreased the anodic dissolving rate of iron and the cathodic hydrogen evolution reaction rate, according to the findings of the polarisation test. EIS data demonstrated that the presence of LTLE raises the R_p values while decreasing C_{dl} valuesand 93.51% inhibition efficiency obtained. In addition, the adsorption characteristics of all studied LTLE were related to the Langmuir adsorption isotherm. The reduced (negative) ΔG^o_{ads} values are attributed to the spontaneous adsorption and exothermic inhibition performance, and the protective coating formed on the surface of the soft steel.Chemisorption and physisorption play a vital role in LTLE adsorption on the soft steel surface. The solution site of the film has a hydrophobic character. The FT-IR spectra of pure LTLE and soft steel submerged in 1M HCl, along with LTLE, reveal the complex formation with Fe ions from soft steel and the components in the LTLE. The SEM images revealed that in the absence of the inhibitor the soft steel surface was severely affected by the acid solution, but in the presence of LTLE inhibitor the surface was strongly protected by the attack of acid solution. AFM studies shows that in presence of LTLE surface roughness was minimum compared to the absence of the inhibitor. The contact angle studies concluded that the components of extract make good hydrophobicity of the soft steel surface. The outcomes from modeling approaches of quantum mechanical computations proved that the DFT findings supported that the efficient electron-rich areas of LTLE molecules are the primary features in their adsorption.

Acknowledgment

The authors acknowledge the Department of Chemistry at KLE Technological University in Hubballi, India, for providing an electrochemical workstation (CH1660E model), and the DST-SAIF University Scientific and Instruments Center in Karnatak University Dharwad for providing SEM and CA spectroscopy capabilities. S. K. Rajappa is grateful and appreciative of the funding provided by the Karnatak University, Dharwad Seed Grant for Research Program.

References

1 Verma D K, Kazi M, Alqahtani M S, Syed R, Berdimurodov E, Kaya S, Salim R, Asatkar A & Haldhar R, *J Mol Struct*, 1241 (2021) 130648.
2 Haque J, Verma C, Srivastava V & Nik W W, *Int J Electrochem Sci*, 8 (2013) 7138.
3 Kairi N I & Kassim J, *Int J Electrochem Sci*, 8 (2013) 7138.
4 Qiang Y, Zhang S, Tan B & Chen S, *Corros Sci*, 133 (2018) 6.
5 Alibakhshi E, Ramezanzadeh M, Bahlakeh G, Ramezanzadeh B, Mahdavian M & Motamedi M, *J Mol Liq*, 255 (2018) 185.
6 Shetty S D, Shetty P & Nayak H V S, *J Serb Chem Soc*, 71 (2006) 1073.
7 Wang H, Fan H & Zheng J, *Mater Chem Phys*, 77 (2002) 655.
8 Hmimou J, Rochdi A, Touir R, Touhami M E, Rifi E H, Hallaoui A E, Anouar A & Chebab D, *J Mater Environ Sci*, 3 (2012) 543.
9 Praveen B M & Venkatesha T V, *Int J Electrochem Sci*, 4 (2013) 267.
10 Leelavathi S & Rajalakshmi R, *J Mater Environ Sci*, 4 (2013) 625.
11 Bentiss F, Traisnel M & Lagrenee M, *Corros Sci*, 42 (2000) 127.
12 Arab S T & Noor E A, *Corros Sci*, 49 (1993) 122.
13 Ramananda S M, *J Mater Environ Sci*, 4 (2012) 119.
14 Taleb H, Ibrahim & Mohamed A Z, *Int J Electrochem Sci*, 6 (2012) 6442.
15 Tiwari P, Srivastava M, Mishra R, Ji G & Plakasi R, *J Environ Chem Eng*, 6 (2018) 4773.
16 Rani A J, Thomas A & Joseph A, *J Mol Liq*, 334 (2021) 116515.
17 Rathod M R, Rajappa S K, Praveen B M & Bharath D K, *Curr Green Sust Chem*, 4 (2021) 100113.
18 Wang Q, Tan B, Bao H, Xie Y, Mou Y, Li P & W Yang, *Bioelectrochemistry*, 128 (2019) 49.
19 Fekkar G, Yousfi F, Elmsellem H, Aiboudi M, Ramdani M, Abdel-Rahman I & Bouyazza L, *Int J Corros Scale Inhib*, 9 (2020) 446.
20 Sedik A, Lerari D, Salci A, Athmani S, Bachari K, Gecibesler H I & Solmaz R, *J Taiwan Inst Chem Eng*, 107 (2020) 189.
21 Haque J, Verma C, Srivastava V & Nik W W, *Sustain Chem Pharm*, 19 (2021) 100354.
22 Fadhil A A, Khadom A A, Ahmed S K, Liu H, Fu C & Mahood H B, *Surf Interfaces*, 20 (2020) 100595.
23 Thomas A, Praiila M, Shainy K M & Joseph A, *J Mol Liq*, 312 (2020) 113369.
24 Ojha L K, Tuzun B & Bhawsar J, *J Bio Tribo Corros*, 6 (2020) 1.
25 Akalezi C O & Oguzie E E, *Int J Ind Chem*, 7 (2016) 81.
26 Rathod M R, Rajappa S K & Kittur A A, *Mater Today: Proc*, 54 (2022) 786.
27 Kumar S, Sharma S & Vasudeva N, *Asian Pac J Trop Dis*, 2 (2012) 761.
28 Sharma V & Rao L J M, *Crit Rev Food Sci Nutr*, 54 (2014) 433.
29 Vimala J R, Rose A L & Raja S, *Der Chemica Sinica*, 3 (2012) 582.
30 Shaikh J R & Patil M K, *Int J Chem Stud*, 8 (2020) 603.
31 Zhang W, Li H, Wang Y, Liu Y, Gu Q & Wu Y, *New J Chem*, 42 (2018) 12649.

32 Hsissou R, About S, Seghiri R, Rehioui M, Berisha A, Erramli H, Assouag M & Elharfi A, *J Mater Res Technol*, 9 (2020) 2691.
33 Merah S, Larabi L, Benali O & Harek Y, *Pigm Resin Technol*, 37 (2008) 291.
34 Fouda A S, Ibrahim H, Rashwaan S, El-Hossiany A & Ahmed R M, *Int J Electrochem Sci*, 13 (2018) 6327.
35 Sasikala T, Parameswari K, Chitra S & Kiruthika A, *Measurement*, 101 (2017) 175.
36 Rathod M R & Rajappa S K, *Electrochem Sci Adv*, (2021) e2100059.
37 Prasanna B M, Praveen B M, Hebbar N, Venkatesha T V & Tandon H C, *Int J Ind Chem*, 7 (2016) 9.
38 Ituen E B, Akaranta O, James A O & Shuangqin S, *J Chem Mater Res*, 5 (2016) 45.
39 Singh A K & Ebenso E E, *Int J Electrochem Sci*, 7 (2012) 2349.
40 Haldhar R, Prasad D, Nguyen L T D, Kaya S, Bahadur I, Dagdag O & Kim S, *Mater Chem Phys*, 267 (2021) 124613.
41 Rathod M R & Rajappa S K, *Electrochem Sci Adv*, 2 (2021) e2100080.
42 Martinez S & Matikos-Hukovic M, *J Appl Electrochem*, 33 (2003) 1137.
43 Ostovari A, Hoseinieh S M, Peikari M, Shadizadeh S R & Hashemi S J, *Corros Sci*, 5 (2009) 1935.
44 Ahamad I, Prasad R & Quraishi M A, *J Solid State Electrochem*, 14 (2010) 2095.
45 Dandia A, Gupta S L, Singh P & Quraishi M A, *ACS Sustain Chem Eng*, 1 (2013) 1303.
46 Langmuir I, *J Am Chem Soc*, 38 (1916) 2221.
47 Zarrouk A, Hammouti B, Dafali A, Bentiss F & Oujda M, *Ind Eng Chem Res*, 52 (2013) 2560.
48 Solomon M M, Umoren S A, Udosoro I I & Udoh A P, *Corros Sci*, 52 (2010) 1317.
49 Outirite M, Lagrenee M, Lebrini M, Traisnel M, Jama C, Vezin H & Bentiss F, *Electrochim Acta*, 55 (2010) 1670.
50 Rathod M R, Minagalavar R L & Rajappa S K, *J Indian Chem Soc*, 99 (2022) 100445.
51 Devendra B K, Praveen B M, Tripathi V S, Nagaraju G, Nagaraju D H & Nayana K O, *Inorg Chem Commun*, 134 (2021) 109065.
52 Kalkhambkar A G, Rajappa S K, Manjanna J & Malimath G H, *J Indian Chem Soc*, 99 (2022) 100639
53 Guruprasad A M, Sachin H P, Swetha G A, Prasanna B M & Sudheerkumar K H, *J Bio Tribo Corros*, 4 (2018) 57.
54 Rathod M R, Rajappa S K, Minagalavar R L, Praveen B M, Devendra B K & Kittur A A, *Inorg Chem Commun*, 140 (2022) 109488.
55 Ekemini I, Victor M & Ekere E, *Colloids Surf A*, 578 (2019) 123597.
56 Dehghani A, Bahlakeh G, Ramezanzadeh B & Ramezanzadeh M, *J Taiwan Inst Chem Eng*, 102 (2019) 349.
57 Su H, Wang L, Wu Y & Zhang Y, *Corr Sci*, 165 (2020) 108410.
58 Qiang Y, Zhang S, Guo L & Zheng X, *Corr Sci*, 119 (2017) 68.
59 Obot I B, Macdonald D D & Gasem Z M, *Corr Sci*, 99 (2015) 1.
60 Madkour L H, Kaya S, Kaya C & Guo L, *J Taiwan Inst Chem Eng*, 68 (2016) 461.
61 Huang H & Bu F, *Corr Sci*, 165 (2020) 108413.
62 Haddadi S A, Alibakhshi E & Bahlakeh G, *J Mol Liq*, 284 (2019) 682.
63 Hu S, Jia X & Hu J, *J China Univ Petrol*, 35 (2011) 146.
64 Kalkhambkar A G, Rajappa S K, Manjanna J & Malimath G H, *Inorg Chem Commun*, 143 (2022) 109799.
65 Sanaei Z, Ramezanzadeh M, Bahlakeh G & Ramezanzadeh B, *J Ind Eng Chem*, 69 (2019) 18.
66 Bahlakeh G, Dehghani A, Ramezanzadeh B & Ramezanzadeh M, *J Mol Liq*, 294 (2019) 111550.